Journal of Membrane Science 380 (2011) 199–207

Contents lists available at ScienceDirect

Journal of Membrane Science

journal homepage: www.elsevier.com/locate/memsci

Proton diffusion in polyelectrolytes based on hydrogenated polynorbornenes with imide side groups in the repeat unit as determined by NMR and impedance spectroscopies

Leoncio Garrido[a], Mar López-González[a], Mikhail Tlenkopatchev[b], Evaristo Riande[a,*]

[a] Instituto de Ciencia y Tecnología de Polímeros, CSIC, 28006 Madrid, Spain
[b] Instituto de Investigaciones en Materiales, UNAM, Mexico DF, Mexico

ARTICLE INFO

Article history:
Received 9 August 2010
Received in revised form 6 June 2011
Accepted 1 July 2011
Available online 7 July 2011

Keywords:
Proton exchange membranes
Polynorbornenes
Pulsed field gradient NMR

ABSTRACT

The conductivity of sulfonated membranes based on hydrogenated polynorbornene functionalized with dicarboximide side groups, specifically hydrogenated poly(exo,endo-*N*-phenyl-norbornene-5,6-dicarboximide), was determined by impedance spectroscopy in the temperature range 10–40 °C. Using Nernst–Planck transport equations, the diffusion coefficient of protons in the membranes was estimated. The diffusion of protons was also measured by pulsed field gradient (PFG) NMR techniques at several temperatures. The comparison of the temperature dependence of the diffusion coefficients of protons obtained by the two techniques suggests that a vehicular type mechanism governs the transport. Solid state ^{23}Na magic angle spinning (MAS) NMR was used to determine the state of sodium counterions in membranes equilibrated with 1 M sodium chloride solutions. The spectra exhibit two peaks, one narrow and another broad, corresponding, respectively, to isolated hydrated sodium ions and clustered sodium ions.

1. Introduction

The study of the electrochemical characteristics of proton exchange membranes (PEM) in terms of the chemical structure is a subject of great interest in the efforts toward the improvement of the properties of solid electrolytes separating the fuel from the oxidant in fuel cells. PEMs should exhibit stable chemical properties to overcome the unfriendly oxidative degradation in fuel cell operating conditions [1,2]. Also, the mechanical properties of PEMS should be good enough to allow the fabrication of membrane-electrode assemblies (MEAs). Aside from these important characteristics, high performance proton exchange membranes should display high protonic conductivity and negligible electronic conductivity. The strong dependence of polymeric acidic membranes on water content precludes their use at temperatures above 100 °C, thus impeding the utilization of low quality platinum catalyst in low temperature fuel cells technology. To develop systems that can conduct protons with little or no water content is one of the greatest challenges facing fuel cell membranes technology [3].

The conductive process presumably involves dissociation of the proton from the acidic site of the membranes by the action of water, subsequent transfer of the proton to the aqueous medium, screening of the hydrated proton from the conjugated base or fixed anion, and finally diffusion of the proton in the confined water within the polymer matrix [4]. The distribution of water in membranes may be inhomogeneous under operating conditions due to electro-osmotic drag of water from the anode to the cathode and/or back diffusion of the water produced in the cathode to the anode. These facts in conjunction with water evaporation and change of the water content caused by membrane electrode assembly, strongly affect the conductivity of membranes. As a consequence, to know the water profile across PEMs in working conditions requires the knowledge of the electro-osmotic permeability and the diffusion coefficient of water in the acidic ion-exchange membranes [5–7].

The estimation of the proton conductivity in membranes provides an indirect way of determining the diffusion coefficient of protons in the case that all protons in the membranes intervene in the conductive process. On the other hand, pulsed field gradient (PFG) NMR techniques have been widely used to study molecular diffusion of fluids in confined and non-confined geometries [8,9]. The technique has also been extended to determine apparent diffusion constants of protons in acidic ion-exchange membranes with different water uptake [10–15]. At first sight, a comparison of the proton diffusion coefficients obtained from conductivity and PFG NMR techniques may shed light on the transport mechanisms in membranes.

* Corresponding author. Tel.: +34 91 5622900; fax: +34 91 5644853.
E-mail address: riande@ictp.csic.es (E. Riande).

0376-7388/$ – see front matter © 2011 Elsevier B.V. All rights reserved.
doi:10.1016/j.memsci.2011.07.001

Polynorbornenes exhibit excellent properties for dielectric applications, such as interval dielectrics in microelectronics, and for gas separation and packaging. In the literature, norbornene monomers with alkyl [16] or fluoroalky [17] side groups have been reported that were further polymerized via ring opening polymerization metathesis on bicycloolefins to yield polymer chains with cyclolinear backbone. More recently, Tlenkopatchev and coworkers [18–20] functionalized norbornenes with dicarboximide groups which were further modified by substituting the hydrogen of the imide group with different moieties such as phenyl, cyclohexyl, adamantly, etc. groups, giving rise to novel polymers differing in physical properties. Membranes were cast from modified polynorbornene solutions and a systematic study was carried out on the properties of these membranes in gas separation [21–24]. This novel type of polymers allows anchoring different types of moieties to the imide groups that can be further sulfonated to obtain new cation-exchange membranes. The aim of this paper was to study with PFG NMR the ^{1}H intradiffusion coefficient in this type of membranes, paying special attention to the effect of the ion-exchange capacity and water content on proton transport. In parallel, the diffusion coefficient of protons attached to the fixed ionic groups accounting for the proton conductivity was estimated from conductivity measurements using Nernst–Planck type equations. The comparison of the diffusion coefficients of protons estimated by PFG NMR and conductivity may provide information concerning proton transport in the membranes.

In addition, since solid state ^{23}Na magic angle spinning (MAS) NMR can directly observe sodium ions, this technique has been used to obtain information on the local environment of fixed ions (anions or cations) bound to ionomers [25]. With this technique, it is possible to identify the presence of isolated, hydrated and clustered sodium ions in sulfonated polymers based upon differences in their chemical shifts. Here, ^{23}Na MAS NMR was used to study the state of free ions or counterions in neutralized polynorbornene based cation-exchange membranes.

2. Experimental

2.1. Cation-exchange membranes

Poly(*N*-phenyl-exo,endo-norbornene-5,6-dicarboximide) (PPhNDI) was synthesized by ring-opening metathesis polymerization of *N*-phenyl-exo,endo-norbornene-5,6-dicarboximide as indicated elsewhere [26]. The values of the number-average molecular weight, M_n, polydispersity index, M_w/M_n, and glass transition temperature were, respectively, 2.1×10^5, 1.3 and 222 °C. The double bonds of the norbornene residues in PPhNDI were hydrogenated at room temperature using pressures ranging from 1 to 115 bars, employing suitable catalysts. The hydrogenated polymer (PPhHNDI) was further sulfonated in dichloromethane solution with acetyl sulfate in an ice bath. By varying the sulfonation time two polyelectrolytes soluble in common organic solvents such as dimethyl sulfoxide, dimethylformamide, and *N*,*N*-dimethylacetamide, were obtained. A scheme of the repeating unit of the polyelectrolytes is shown in Fig. 1. Cation-exchange membranes (SPPhHNDI) were cast from solutions of the polyelectrolytes in dimethyl sulfoxide.

2.2. Water uptake and ion-exchange capacity of membranes

Water uptake was obtained from the weights of dry- and water-equilibrated membranes. The ion exchange capacity of the membranes was obtained by equilibrating the membrane in the acidic form with a 1 M sodium chloride solution. The hydrochloric acid liberated in the interchange reaction

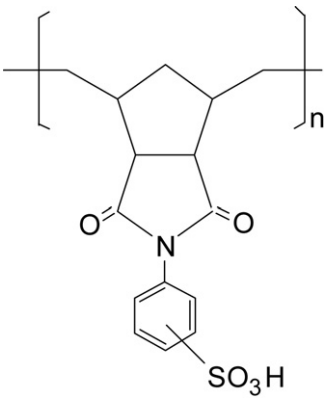

Fig. 1. Repeating unit hydrogenated poly(*N*-phenyl-exo,endo-norbornene-5,6-dicarboximide), partially sulfonated.

$$R\text{–}H + Na^+ \rightarrow R\text{–}Na + H^+$$

was titrated with a 0.01 M sodium hydroxide solution. The values of the water uptake in g H_2O/(g dry membrane) and ion-exchange capacity (IEC) in mequiv. H^+/(g dry membrane) were, respectively, 0.187 and 0.64 for the membrane with acronym SPPhHNDI1 and 0.284 and 1.18, respectively, for the membrane with acronym SPPhHNDI2.

2.3. Conductivity measurements

The complex impedance of the membranes in the acid form, equilibrated with distilled water, was measured at different temperatures ranging from 10 to 40 °C. The measurements were performed with a Novocontrol broadband dielectric spectrometer (Hundsagen, Germany) integrated by a SR 830 lock-in amplifier with an Alpha dielectric interface in the frequency range 10^{-2}–10^6 Hz. The electrodes used were gold disks of 10 mm of diameter. The temperature was controlled by a nitrogen jet (QUATRO from Novocontrol) with a temperature error of 0.1 K during every single sweep in frequency.

2.4. NMR measurements

The NMR experiments were performed in a Bruker Avance™ 400 spectrometer equipped with a 89 mm wide bore, 9.4 T superconducting magnet (Larmor frequencies of proton and ^{23}Na at 400.13 and 105.86 MHz, respectively).

To determine the diffusion coefficients of water in the SPPhHNDI membranes with NMR, the samples were initially hydrated overnight by immersion in distilled water, blotted to remove droplets and transferred to a 5 mm o.d. NMR tube and closed with a plastic cap and wrapped with paraffin film. In successive steps, water in the membrane was partly evaporated in a controlled atmosphere until the reported concentration was reached. In all cases, the proton NMR measurements were performed after allowing 12 h for equilibration of moisture within the tube volume. Samples were weighted with a precision of 0.1 mg before and after measurements and no significant weight loss was observed (<1%).

The proton diffusion reported data were acquired at 15, 25 and 35 ± 1 °C with a Bruker diffusion probehead Diff60 using 90° ^{1}H pulse lengths between 6.0 and 6.5 μs. A pulsed field gradient stimulated spin echo pulse sequence illustrated in Fig. 2 was used. The echo time between the first two 90° rf pulses, τ_1, was 2.71 ms. The apparent diffusion coefficient of protons, D_{app}, was measured at several diffusion times, Δ, with gradient pulses of 1.6 ms, and vary-

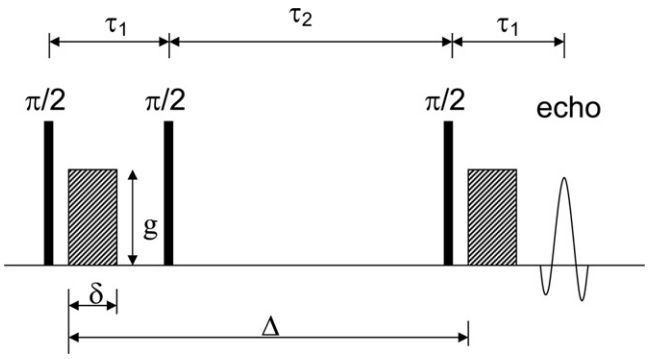

Fig. 2. Sketch of pulse sequence used in the PFG NMR experiments.

ing their amplitude between 0 and 14 T m^{-1}. The diffusion time was varied from 10 to 40 ms and the repetition rate was 3 s. The total acquisition time for these experiments varied from 15 to 80 min. The decay of the echo amplitude was monitored typically to, at least, 35% of its initial value and the apparent diffusion coefficient at a given Δ was calculated by fitting a stretched exponential function to the decay curve.

Previously, the gradient was calibrated according to the spectrometer manufacturer protocol, using a sample of water doped with $CuSO_4$ at 1.0 g L^{-1} and a value of the water diffusion coefficient equal to 2.3×10^{-9} m^2 s^{-1}. Furthermore, the calibration was verified at the range of gradient values used experimentally by measuring the diffusion coefficient of dry glycerol. It was found a value of $D = 2.23 \times 10^{-12}$ m^2 s^{-1}, in good agreement with those reported [27].

The ^{1}H longitudinal relaxation times, T_1, of water in membranes were estimated using an inversion-recovery (π–t_i–$\pi/2$) pulse sequence.

The solid state ^{1}H and ^{23}Na NMR spectra were acquired with a standard Bruker double resonance 4 mm cross-polarization/magic angle spinning NMR probehead using ~35° ^{1}H and ^{23}Na pulse lengths between 1.0 and 2.0 μs, and recycle delays of 5 and 20 s, respectively. Samples were placed in 4 mm zirconia rotors and spun at the magic angle at a rate of 8.0 kHz. For the ^{23}Na NMR spectra, high power proton decoupling was used. The ^{1}H and ^{23}Na spectra were externally referenced to TMS and 1 M sodium chloride solution, respectively.

3. Results

3.1. Conductivity measurements

The equivalent electrical circuit for ideal acidic membranes is an ohmic resistance R_0 that accounts for the proton ohmic resistance in series with a parallel *RC* circuit where *R* and *C* represent respectively the polarization resistance and the capacitance of the membrane. For real membranes the capacitor must be replaced by a constant phase element (CPE) with admittance $Y^*(\omega) = Y_0(j\omega\tau)^n$ with $0 < n \leq 1$, where τ denotes an average relaxation time [28]. The complex impedance of the circuit is given by

$$Z^*(\omega) = R_0 + \frac{R}{1 + Y_1(j\omega\tau)^n} \quad (1)$$

here $Y_1 = RY_0$ is a dimensionless quantity. An inspection of Eq. (1) shows that for the $Z''(\omega)$ *vs.* $Z'(\omega)$ plot or Nyquist diagram, the following conditions for the frequency limits hold

$$\begin{aligned} &\lim_{\omega\to\infty} Z'(\omega) = R_0; \quad \lim_{\omega\to\infty} Z''(\omega) = 0 \\ &\lim_{\omega\to 0} Z'(\omega) = R; \quad \lim_{\omega\to 0} Z''(\omega) = 0 \end{aligned} \quad (2)$$

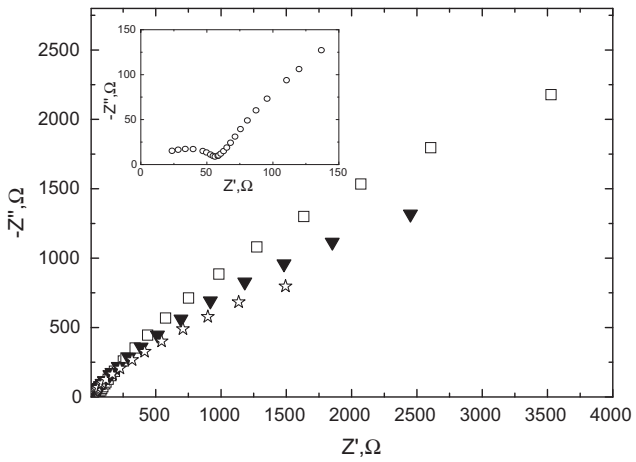

Fig. 3. Nyquist plots at 10 °C (□), 25 °C (▼) and 40 °C (☆). Inset: details of the experimental data at high frequencies, at 10 °C.

Accordingly, the intersection of the $Z''(\omega)$ *vs* $Z'(\omega)$ curve with the abscissa axis yields R_0. An illustrative Nyquist plot for the SPPhHNDI1 membrane equilibrated with water, illustrated in Fig. 3, exhibits two curves where the high- and the low-frequency sides of the low- and high-frequency curves intersect with the abscissa axis, respectively, at the same point. In principle, the ohmic resistance of the membrane is assumed to be the value of the real impedance at the intersection point. Then, the equivalent circuit modeling the impedance of the membrane sandwiched between the electrodes consists of a constant phase element CPE1 in parallel with the equivalent circuit of the membrane described by Eq. (1) (see Fig. 4). At low frequencies, Eq. (1) describes the impedance arising from the polarization of the membrane whereas at high frequencies the polarization is nil and the impedance is modeled by the ohmic resistance of the membrane in parallel with the constant phase element CPE1.

An alternative and often more convenient method to analyze the impedance results is the Bode diagram that involves the plot of the modulus of the impedance, $|Z^*(\omega)|$, against frequency. In this case, at the extreme frequencies, it is obtained that

$$\begin{aligned} &\lim_{\omega\to\infty} |Z^*(\omega)| = R_0; \quad \lim_{\omega\to\infty} \phi(\omega) = 0 \\ &\lim_{\omega\to 0} |Z^*(\omega)| = R_0 + R_p; \quad \lim_{\omega\to 0} \phi(\omega) = 0 \end{aligned} \quad (3)$$

where $\phi = \tan^{-1}[Z''(\omega)/Z'(\omega)]$. Bode diagrams for the SPPhHNDI1 and SPPhHNDI2 membranes saturated with water are shown at several temperatures in Figs. 5 and 6, respectively. As usual, the curve representing the evolution of the modulus of the impedance with frequency exhibits a plateau at low frequencies. However, as frequency increases $|Z^*(\omega)|$ drops reaching a second plateau that slightly decreases with increasing frequency. The value of $|Z^*(\omega)|$ in the second plateau at which $\phi(\omega)$ reaches a maximum is taken as the ohmic resistance of the membrane, R_0. Notice a significant

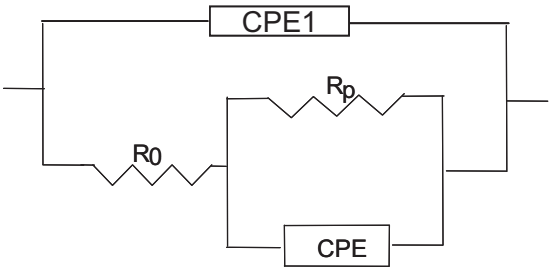

Fig. 4. Equivalent circuit of the acidic SPPhHNDI1 membrane sandwiched between electrodes.

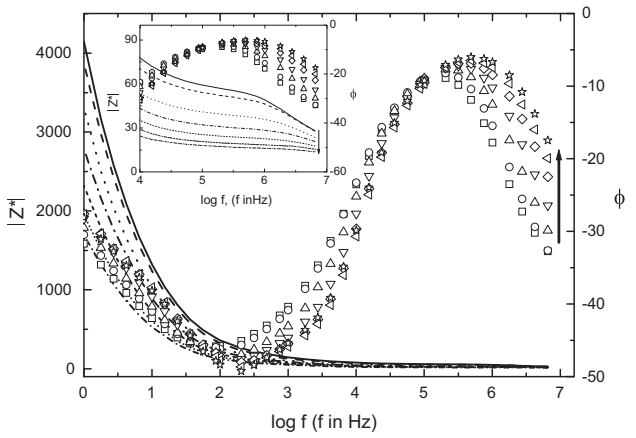

Fig. 5. Bode diagram for the PPhHNDI1 membrane equilibrated with water from 10 °C (□ for ϕ and solid line for $|Z^*(\omega)|$) to 40 °C (□ and short dash dot lines) in steps of 5 °C, increasing the temperature in the direction indicated by the arrows shown in the figure. Inset: details of the diagram at high frequencies.

decrease in $|Z^*(\omega)|$ at frequencies above those associated with ϕ_{max} corresponding to the high frequency curve in the Nyquist diagrams. The proton conductivity of the membranes, σ, was obtained from R_0 by means of the following expression

$$\sigma = \frac{l}{R_0 S} \tag{4}$$

where S and l are, respectively, the area and thickness of the membranes. In general, the values of conductivities obtained from Nyquist and Bode diagrams are rather close, the difference between them being only of a few percents; for example the values of this quantity determined from Nyquist and Bode diagrams are 3.5×10^{-4} and 3.9×10^{-4} S/cm for the SPPhHNDI1 membrane, at 40 °C. In what follows the values of R_0 obtained from Bode diagrams were used and the corresponding proton conductivities of the SPPhHNDI1 and SPPhHNDI2 membranes saturated with water, at several temperatures, are collected in Tables 1 and 2, respectively.

3.2. ^{1}H PFG NMR measurements

PFG NMR methods to measure diffusion of protons in cation-exchange membranes are based on the relationship between the resonance frequency of the nucleus of interest and the external magnetic field it experiences, as expressed by the Larmor equation: $\omega_0 = -\gamma B_0$. The application of a magnetic field gradient across the sample volume labels magnetically molecules having NMR sensitive nuclei enabling the tracking of their motion over a given time, the diffusion time. In practice, this is accomplished using a spin echo type of pulse sequence, as first described by Stejskal and Tanner [29]. In the present work, a PFG stimulated spin echo sequence shown in Fig. 2 was used. The application of three consecutive and suitably spaced $\pi/2$ radiofrequency (rf) pulses generates an observable NMR signal (echo) centered at a time equal to $2\tau_1 + \tau_2$ from the first rf pulse, where τ_1 is the time separation between the first two rf pulses and τ_2 is the time elapsed between the second and the third rf pulses. The magnetic labeling is accomplished by applying two gradient pulses of amplitude and duration g and δ, respectively, spaced by a time Δ, the diffusion time. In the absence of motion, the loss of phase coherence of the NMR signal caused by the first gradient pulsed would be compensated by the second gradient pulse, but this would not be the case if molecular diffusion occurs during the time Δ. Then, an attenuation of the echo is observed as expressed by

$$A(g) = A(0)\exp(-bD) \tag{5}$$

where $A(g)$ and $A(0)$ are the amplitude of the echo in the presence of a gradient pulse with amplitude g and 0, respectively, $b = (\gamma g \delta)^2 (\Delta - \delta/3)$ where γ is the gyromagnetic ratio of the nucleus being observed, and D is the diffusion coefficient. Knowing D and considering that the mean square displacement in one dimension is given by

$$\langle x^2 \rangle = 2D\Delta \tag{6}$$

the PFG NMR measurements allow probing the membrane morphology at molecular level and its effect upon transport properties.

Prior to performing the diffusion measurements, the proton signal corresponding to water absorbed in the membranes was analyzed. The results are summarized in Table 3. A single peak was detected at ~4.8 ppm and the lineshape was broad, varying the peak full-width at half-height, $\nu_{1/2}$, from 230 to 430 Hz with decreasing water content, from 0.195 to 0.094 g H_2O/(g dry membrane), respectively. The broadening could be attributed partly to the heterogeneity of the protons environment and residual amounts of transition metal-based catalyst used in the synthesis of the polymer still present in the membrane. As a consequence, the effective

Table 1
Resistance, R_0, conductivity, σ and diffusion coefficients of protons, $D(H^+)$, for the membrane SPPhHNDI1 at several temperatures.

T, °C	R_0, Ω[a]	$\sigma \times 10^4$, S/cm	$D(H^+) \times 10^{12}$, m^2 s^{-1}
10	56.79	1.14	4.93
20	39.30	1.65	7.39
30	23.41	2.77	12.83
40	16.57	3.92	18.76

[a] The area and thickness of the membranes are 0.7854 cm^2 and 51 ± 3 μm, respectively

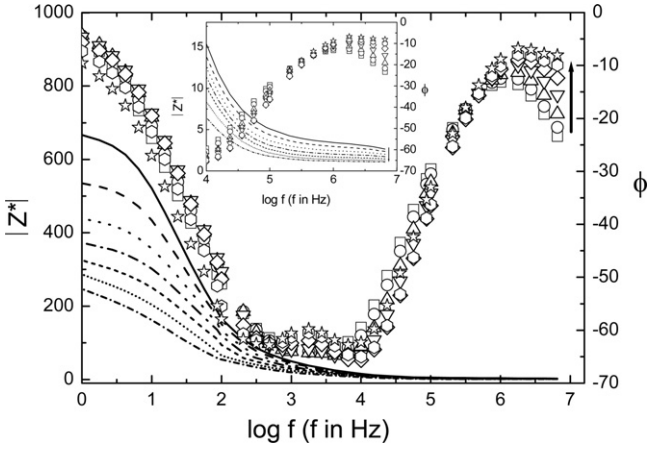

Fig. 6. Bode diagram for the PPhHNDI2 membrane equilibrated with water from 10 °C (□ for ϕ and solid line for $|Z^*(\omega)|$) to 40 °C (□ and short dash dot lines) in steps of 5 °C, increasing the temperature in the direction indicated by the arrows shown in the figure. Inset: details of the diagram at high frequencies.

Table 2
Resistance, R_0, conductivity, σ and diffusion coefficients of protons, $D(H^+)$, for the membrane SPPhHNDI2 at several temperatures.

T, °C	R_0, Ω[a]	$\sigma \times 10^3$, S/cm	$D(H^+) \times 10^{10}$, m^2 s^{-1}
10	3.44	3.78	0.97
20	2.36	5.50	1.46
30	1.62	8.02	2.19
40	1.16	11.20	3.16

[a] The area and thickness of the membranes are 0.7854 cm^2 and 102 ± 3 μm, respectively.

transverse or spin-spin relaxation time, $T_2^* = 1/\pi\nu_{1/2}$, of protons in these membranes is short. On the other hand, the T_1 measurements showed an increase from 140 to 230 ms with a reduction in water content from 0.195 to 0.094 g H_2O/(g dry membrane), respectively. Since the PFG methods are based on the observation of an echo, the rapid decay of the proton signal (short T_2^*) leads to a significant reduction in the signal-to-noise ratio of the spectrum, thus limiting the practical range of some experimental parameters, *i.e.,* diffusion times, and requiring an increase in signal averaging to improve detection. Thus, a stimulated spin echo sequence was chosen because it allows short echo times and the diffusion time is limited by T_1. The proton signal of membranes saturated by immersion in an aqueous solution of NaCl was ~23% higher than the signal corresponding to those saturated in distilled water. A proton signal loss of about 2.5% was measured 24 h after placing the membrane in a NMR capped tube. Proton spin echo signals in dried membranes were not observed.

The diffusion data fit well to a monoexponential function in membranes with high water content. However, an increasing deviation from a monoexponential fit with decreasing water content was observed. Since a continuum spectrum of diffusion coefficients might be a more realistic description of the systems under consideration than that provided by a set of discrete values (*i.e.* multiexponential fit), the data were fitted to a stretched exponential

$$A(g) = A(0)\exp[-(bD_{app})^{\beta}] \quad (7)$$

where β is a "stretch" parameter lying in the range $0 < \beta \leq 1$, D_{app} is the apparent diffusion coefficient and the rest of the variables as previously described. Fig. 7a and b illustrates the results of the monoexponential and stretched exponential fits in SPPhHNDI2 with a water content of 0.195 and 0.10 g H_2O/(g dry membrane), respectively. The results of PFG NMR measurements at various temperatures are summarized in Table 4. It is observed that the values of D_{app} are very sensitive to the water content and ion-exchange capacity of the membranes. Thus, considering a Δ of 20 ms, a reduction in water content of 36% and 49% in the SPPhHNDI1 and SPPhHNDI2 membranes, respectively, decreases the value of the diffusion coefficient at 25 °C in 19% and 33%, respectively. At the same time, in membranes with approximately the same water content, an increase of the ion-exchange capacity from 0.64 to 1.81 mequiv. $[H^+]$/(g dry membrane) leads to a ~10 times increase in the value of D_{app}.

A small influence of the diffusion time upon the values of the proton diffusion coefficients is noted. At fixed ion-exchange capacity, a nearly constant or slight decrease in the values of D_{app} with increasing diffusion time is observed, although the reduction seems more evident at low water contents.

The Arrhenius activation energy associated to the proton diffusion process in these membranes was found to increase from 5.5 to 13.4 kcal/mol with water content decreasing from 0.195 to 0.094 g H_2O/(g dry membrane), respectively.

The values of the stretching parameter β seem to decrease with decreasing water content and appear to be independent of the diffusion time, at least within the time interval studied. In membranes with high water content, the value of β is about 1. The effect of temperature on β is observed in membranes with water content of less than 15%, and its value increases up to an average value of 0.87 with T increasing from 15 to 35 °C. In the evaluation of these results, it should be pointed out that the membrane having 9.4% water content exhibited the highest uncertainties of all measurements performed, as shown in Table 4 (column six). This is due partly to the fact that the corresponding proton spectra showed the widest linewidths measured in the study and, consequently, leading to data with poor signal-to-noise ratio.

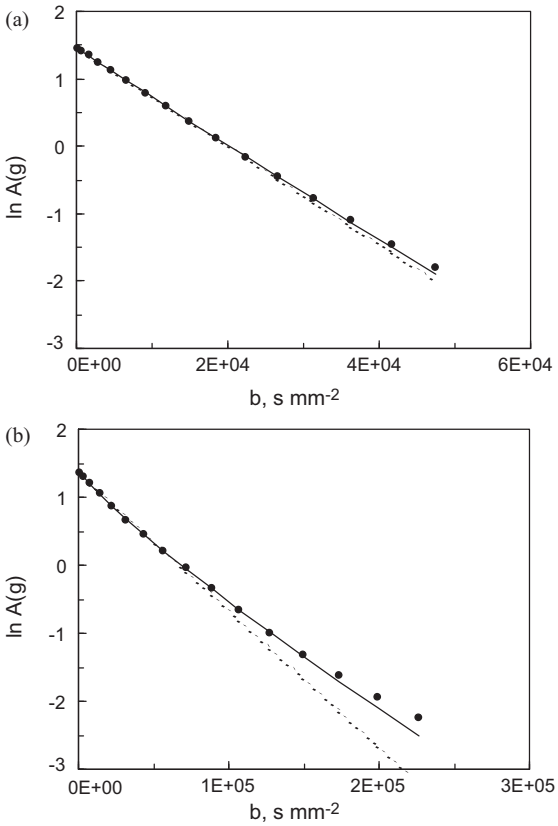

Fig. 7. Plot of $A(g)$ (arbitrary units) *vs.* b (s mm^{-2}) corresponding to water protons in SPPhHNDI2 obtained at 25 °C with a diffusion time, Δ, equal to 40 ms and water content of 19.5% (a) and 10.0% (b). The duration of the gradient pulse, δ, was kept constant to 1.6 ms and the amplitude of the field gradient, g, in T m^{-1}, was varied between 0.16 and 5.60. The dashed (- - -) line corresponds to a mono-exponential (Eq. (5)) fit and the solid line represents the fit to a fractional exponential (Eq. (7)).

3.3. Solid state ^1H and ^{23}Na NMR

The quadrupole moment possessed by nuclei with spin quantum number $I > ½$ interacts strongly with the electric field gradients surrounding the nucleus and, generally, dominates its spectrum line shape and the relaxation behavior. Consequently, this interaction is sensitive to the type of atoms and molecules nearby the observed nucleus, as well as by the formation of complexes. To observe the distribution of sodium ions by ^{23}Na NMR in the polymer membranes, the ion-exchange was performed by immersing the membrane in a 1 M NaCl solution overnight, removed from the solution and blotted to remove liquid droplets on the surface. Fig. 8 shows the ^{23}Na NMR spectra corresponding to wet and dried membrane samples. A narrow peak at 7.6 ppm with a linewidth of 300 Hz is observed in both spectra. This resonance is associated to the presence of isolated sodium ions [25]. Also present is a broad peak centered at −6.0 ppm in the spectrum corresponding to a wet sample that shifts to −10.6 ppm after drying. This peak is attributed to the presence of clustered sodium ions and the shift may be caused by the removal of hydration water. Hydrated sodium ions as present in a sodium chloride aqueous solution exhibit a single narrow peak at 0 ppm (data not shown).

The removal of water in the membranes after drying is illustrated by solid state proton MAS spectrum of the wet and dried membranes as shown in Fig. 9. The resonance associated to water protons at 4.2 ppm is only present in the spectrum of the wet sample.

Table 3
Linewidth and T_1 relaxation time measurements of water protons absorbed in SPPhHNDI membranes at 15 °C.

Sample	Water content, g/(g dry membrane) (%)	IEC, mequiv. H^+/(g dry membrane)	Linewidth (Hz)	T_1[a] (ms)
SPPhHNDI1	14.6	0.64	280	160 (20)
	9.4		430	230 (14)
SPPhHNDI2	19.5	1.18	230	140 (10)
	10.0		340	145 (10)

[a] Standard deviation in parenthesis.

4. Discussion

In general, reaching steady state values for D_{app} measured with PFG NMR depends on the heterogeneity and mobility of the chains through which the diffusive process takes place [30]. For example, steady values of D_{app} are obtained for the diffusion of CO_2 in rubbery materials at $\Delta = 10$ ms, but diffusion times of about 40 ms are needed for obtaining steady diffusion of this gas in polycarbonate glassy membranes. It should be noted that in these latter membranes the diffusive gas species wander in microcavities until fluctuations of local segments of the membranes produce channels of suitable radii through which the gas molecules slide to nearby cavities. Therefore, the distribution of cavities at the local structure of the membranes in conjunction with the local fluctuations govern the diffusion and, as a result, it is necessary to get spin echo responses over larger trajectories what implies larger values of Δ. To achieve steady values of D for CO_2 in composite polysulfone membranes containing ZIF-8 fillers requires diffusion times close to 1 s [31]. Substantial diffusion times are also necessary to obtain steady values of the diffusion coefficient of water protons in acidic ion-exchange membranes owing to the wide variety of hydrophilic/hydrophobic environments. It would be expected that an increase in the heterogeneity of the membranes arising from segregation of hydrophilic moieties from hydrophobic ones will also increase the diffusion time required for obtaining steady values of D_{app}. The apparent diffusion coefficient of protons in Nafion obtained by PFG NMR [13] drops rather sharply with increasing values of Δ at low values of diffusion times (Δ between 4 and 10 ms) and, then, the decrease is moderate reaching steady value at $\Delta \cong 40$ ms in most cases. However, an inspection of the values of D_{app} for the SPPhHNDI1 and SPPhHNDI2 membranes, presented in Table 4, shows that the values of this quantity decrease as Δ increases in such a way that steady results for D_{app} are not reached at $\Delta = 40$ ms, presumably due to the heterogeneity of environment caused by the rigidity of the chains that hinders effective segregation of hydrophilic an hydrophobic domains. These results suggest that it would be necessary to determine D_{app} at $\Delta > 40$ ms, but measurements with longer diffusion times are hampered by short relaxation times of the absorbed water protons and low signal-to-noise ratio. In view of these circumstances and in order to compare the values of D_{app} with those of $D(H^+)$ obtained from conductivity measurements, a decay function was fitted to the experimental results of D_{app} *vs* Δ for the two membranes with higher water content and the pertinent results are plotted as a function of tem-

Table 4
Diffusion coefficients of water protons in SPPhHNDI membranes measured by PFG NMR at various temperatures (standard deviation in parenthesis).

Sample	Water content, %	T, °C	Δ, ms	$10^{11} \times D_{app}$, $m^2\ s^{-1}$	β
SPPhHNDI1	14.6	15	10	1.04 (0.07)	0.73 (0.07)
			20	0.93 (0.02)	0.81 (0.03)
			40	0.800 (0.001)	0.85 (0.02)
		25	10	1.62 (0.07)	0.79 (0.04)
			20	1.43 (0.04)	0.85 (0.03)
			40	1.29 (0.02)	0.87 (0.02)
		35	10	2.2 (0.1)	0.87 (0.06)
			20	2.05 (0.06)	0.85 (0.03)
			40	1.88 (0.02)	0.87 (0.01)
	9.4	15	10	0.16 (0.02)	1.2 (0.2)
			20	0.11 (0.02)	0.6 (0.1)
			40	0.03 (0.02)	0.3 (0.2)
		25	10	0.29 (0.02)	0.78 (0.07)
			20	0.27 (0.01)	0.77 (0.05)
			40	0.19 (0.01)	0.77 (0.08)
		35	10	0.51 (0.01)	0.86 (0.04)
			20	0.50 (0.01)	0.87 (0.03)
			40	0.40 (0.01)	0.85 (0.03)
SPPhHNDI2	19.5	15	10	5.9 (0.1)	1.05 (0.03)
			20	5.60 (0.02)	1.01 (0.01)
			40	5.36 (0.01)	0.960 (0.003)
		25	10	7.96 (0.04)	1.009 (0.006)
			20	7.69 (0.02)	1.000 (0.003)
			40	7.41 (0.02)	0.967 (0.004)
		35	10	12.0 (0.6)	0.88 (0.05)
			20	10.40 (0.03)	0.994 (0.004)
			40	10.20 (0.06)	0.969 (0.008)
	10.0	15	10	1.76 (0.05)	0.83 (0.03)
			20	1.67 (0.04)	0.83 (0.03)
			40	1.37 (0.02)	0.84 (0.02)
		25	10	2.7 (0.2)	0.84 (0.05)
			20	2.54 (0.06)	0.86 (0.02)
			40	2.16 (0.02)	0.86 (0.02)
		35	10	4.30 (0.2)	0.79 (0.04)
			20	3.69 (0.07)	0.87 (0.02)
			40	3.24 (0.06)	0.90 (0.02)

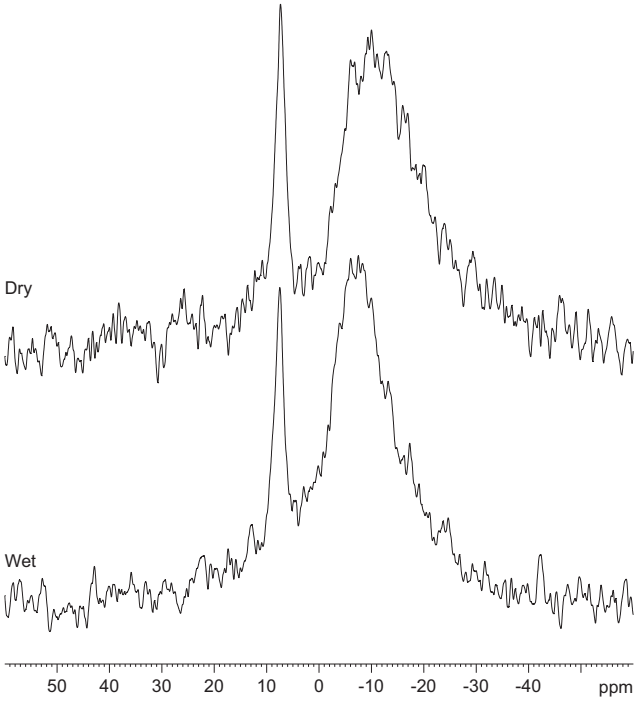

Fig. 8. Solid state ^{23}Na MAS NMR spectra corresponding to wet and dried SPPhHNDI1 membranes, at 25 °C. High power proton decoupling was used and the spectra were externally referenced to the resonance of 1 M sodium chloride solution set at 0 ppm. The narrow peak observed at 7.6 ppm is attributed to the presence of isolated sodium ions. The broad peak centered at −6.0 and −10.6 ppm in the wet and dried samples, respectively, is associated to clustered sodium ions. The right shift observed after drying the sample may be due to the removal of hydration water in the clusters.

perature in Fig. 10. It is expected that these results are close to the real ones and in any case they will be upper-bound values for the apparent diffusion of water protons.

After describing the determination and uncertainties of the values of D_{app}, it is convenient to discuss what it means. In acidic ion exchange membranes equilibrated with water, ^{1}H nuclei

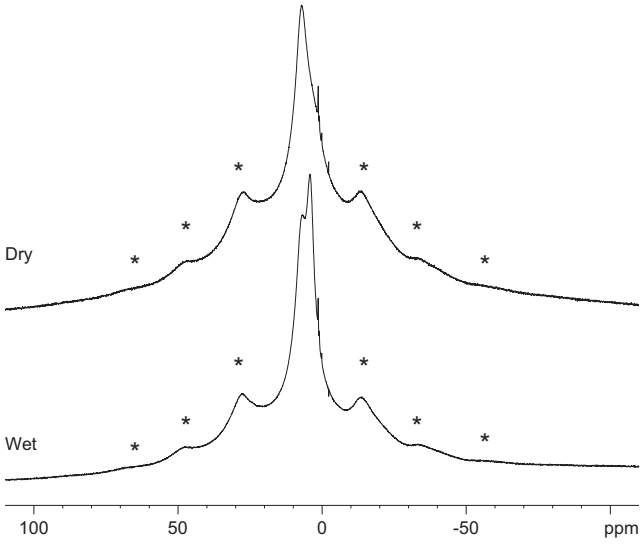

Fig. 9. Solid state ^{1}H MAS NMR spectra corresponding to samples of wet and dried SPPhHNDI1 membranes, at 25 °C. The resonance observed at 4.16 ppm in the wet sample is not present in the dry sample and was assigned to water. The other peaks correspond to the protons present in the polymer chains. The spectra were externally referenced to TMS. The spinning sidebands are indicated by an asterisk.

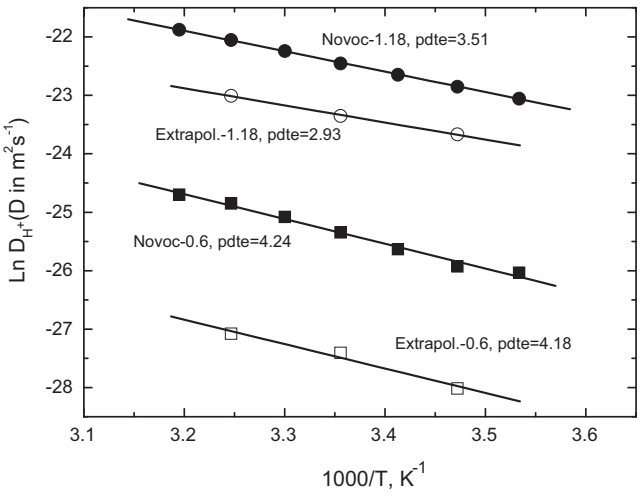

Fig. 10. Arrhenius plots for $D(H^+)$ in SPPhHNDI1 (filled squares) and SPPhHNDI2 (filled circles) membranes saturated with water. Arrhenius plots for $D(^1H)$ in SPPhHNDI1 (open squares) and SPPhHNDI2 (open circles) are also shown; the water contents of the membranes are 0.15 and 0.20 g/g dry membrane, respectively.

exchanges rapidly between water and H^+ where this later ionic specie covers all forms, including aqueous complexes, of H^+ in different environments of the hydrated acidic membrane. As a result, the diffusion coefficient of ^{1}H ($D(^1H) \equiv D_{app}$) is the weighted average of the diffusion coefficients for the separate environments. This consideration suggests that the diffusion coefficient measured by PFG NMR in this work may not exactly be the self-diffusion coefficient of water in the membranes, unless water acts as protons transport. The number of moles of water per fixed ionic group, λ, 16 and 13 for the SPPhHNDI1 and SPPhHNDI2 membranes, is somewhat lower than that displayed by hydrated polyelectrolytes with high conductivity that posses more than 20 mol of water per each fixed ionic group [14,32]. As indicated above, water promotes the formation of hydrophilic and hydrophobic domains in the membranes. The latter domains give mechanical consistence to the membranes whereas the former favor the formation of percolation paths through which proton transport takes place. Segregation and, therefore, formation of percolation paths is easier the higher the flexibility of the molecular chains integrating the membranes is. Recent work [33] carried out on highly hydrated polyimide cation-exchange membranes shows that the diffusion coefficient of protons as measured by PFG NMR spectroscopy, $D(^1H)$, is much lower than $D(H^+)$ for the fully hydrated membranes [15] with high water uptake. The diffusion mechanism in this highly hydrated membranes obeys to the Grotthuss mechanism that involves the proton being handed off from one hydrogen bonding to another one. However, the rather low values of $D(^1H)$ and $D(H^+)$ in the SPPhHNDI membranes presumably are due to the presence of imperfect files of water molecules across the membranes arising from (a) the relatively low ion exchange capacity of the membranes and (b) from the low flexibility of the chains arising from the bulkiness of the functionalized norbornene groups that hinder an efficient segregation of the hydrophilic moieties from the hydrophobic ones. The similarity of $D(^1H)$ and $D(H^+)$ suggests that water moves the proton in the SPPhHNDI membranes and the conductivity mechanism is of vehicle type.

The diffusion coefficient of protons contributing to the proton conductivity may be obtained from Nernst–Planck type equations. In an acidic cation-exchange membrane partially or totally equilibrated with water, electric current under a unidirectional electric force field, $d\psi/dx$, is transported by protons. Neglecting the pore

liquid mobility or convention flow, the flux of protons, J_+, across the membrane is given by [33]

$$J_+ = c_+ u_+ = -c_+ \bar{u}_+ \frac{d\psi}{dx} \quad (8)$$

In this equation, $c_+ = -X^-$, where X^- is the concentration of $-SO_3^-$ ions in the membrane and $\bar{u}_+ = FD(H^+)/RT$ is the ionic mobility of the protons, $D(H^+)$ being the diffusion coefficient of conducting protons. Since the current density is $j = FJ_+$, the electrical conductance can be written as [14,33]

$$\sigma = -\frac{j}{d\psi/dx} = \frac{c_+ F^2 D(H^+)}{RT} \quad (9)$$

where F (=96,480 C) is Faraday's constant.

Values of the diffusion coefficient of protons in SPPhHNDI1 and SPPhHNDI2 membranes saturated with water, obtained from Eq. (9), are shown as a function of temperature in Tables 1 and 2, respectively. Arrhenius plots for these results, shown in Fig. 10, give straight lines from whose slopes activation energies of 8.4 and 7.0 kcal/mol were obtained for the diffusion coefficients of protons, $D(H^+)$, in SPPhHNDI1 and SPPhHNDI2 membranes, respectively. The activation energies associated with $D(^1H)$ obtained from PFG NMR experiments (see Fig. 10) are 8.4 and 5.8 kcal/mol, respectively, for the membranes SPPhHNDI1 (water content: 0.15 g/g dry membrane) and SPPhHNDI2 (water content: 0.20 g/g dry membrane). There are some points that should be highlighted: (a) The values of $D(^1H)$ are somewhat lower than those of $D(H^+)$ presumably as a consequence of the fact that the PFG NMR measurements were carried out in membranes with lower water content than those obtained from conductivity. As the results of Table 4 show, a reduction of 49% in the water content of the SPPhHNDI2 membrane decreases $D(^1H)$ by about 71% for $\Delta = 40$ ms, at 25 °C and (b) the activation energies of the diffusion coefficients obtained by the two techniques are rather close. These facts suggest that proton transport that accounts for the conductivity of the acidic membranes is not governed by the Grotthuss mechanism but it is of vehicular type, *i.e.* acidic protons are transported by water molecules.

Finally, a few comments on the ^{23}Na MAS NMR spectra, which show the presence of two pools of sodium ions, isolated and clustered. The distribution of Na^+ in the membranes could be envisioned as ions located discretely along channels seemingly connecting domains of ion clusters. A comparison between the results provided by conductivity and NMR diffusion measurements suggests that the population of ionic groups in channels is insufficient to provide an efficient bridging between ion clusters and, therefore, facilitate the diffusion of protonated species or H^+ by the Grotthuss mechanism.

5. Conclusions

The rigidity of the chains hinders segregation of hydrophilic moieties from hydrophobic ones making difficult the formation of well defined hydrophilic domains that give rise to the formation of percolation paths through proton transport occurs. As a result, even the membranes with rather high cation-exchange capacity exhibit rather low proton conductivity taken as a basis of comparison membranes with flexible sulfonated side groups such as Nafion. A comparative study of the diffusion coefficient of protons obtained from conductivity and PFG NMR techniques suggests that proton transport in the membranes occurs by a vehicular type mechanism. Finally, the study of the distribution of sodium ions in the membranes equilibrated with 1 M sodium chloride, carried out by ^{23}Na NMR, shows the presence of isolated sodium ions and sodium ions clusters in the membranes, the former presumably being present in narrow hydrophilic channels.

Acknowledgments

This work was supported by the Comisión Interministerial de Ciencia y Tecnología (projects: CTQ2005-04710/BQU and MAT2008-06725-C03-01).

References

[1] M.L. Perry, T.F.J. Fuller, A historical perspective of fuel cell technology in the 20th century , Electrochem. Soc. 149 (2002) S59.
[2] T. Sata, Ion-Exchange Membranes , Royal Society of Chemistry, Cambridge, 2004, p. 69.
[3] B.C.H. Steele, A. Heinzel, Materials for fuel-cell technologies , Nature 414 (2001) 345–352.
[4] S.J. Paddison, Proton conduction mechanisms at low degrees of hydration in sulfonic acid-based polymer electrolyte membranes , Ann. Rev. Mater. Res. 33 (2003) 289–319.
[5] M. Eikerling, Y.I. Kharkats, A.A. Kornyshev, Y.M. Volfkovich, Phenomelnological theory of electro-osmotic effect and water management in polymer electrolyte proton-conducting membranes , J. Electrochem. Soc. 145 (1998) 2684–2699.
[6] S. Motupally, A.J. Becker, J.W. Weidner, Diffusion of water in Nafion 115 membranes , J. Electrochem. Soc. 147 (2000) 3171–3177.
[7] X. Ren, W. Henderson, S. Gottesfeld, Electro-osmotic drag of water in ionomeric membranes – new measurements employing a direct methanol fuel cell , J. Electrochem. Soc. 144 (1997) L2267.
[8] J. Kärger, H. Pfeifer, W. Heink, Principles and applications of self-diffusion measurements by nuclear magnetic resonance , Adv. Magn. Reson. 12 (1988) 1–89.
[9] P.T. Callaghan, Pulsed field gradient nuclear magnetic resonance as a probe of liquid state molecular organization , Aust. J. Phys. 237 (1984) 359–387.
[10] T.A. Zawodzinski, M. Neeman, L.O. Sillerud, S. Gottesfeld, Determination of water diffusion coefficients in perfluorosulfonate ionomeric membranes , J. Phys. Chem. 95 (1991) 6040–6044.
[11] J.R.P. Jayakody, P.E. Stallworth, E.S. Mananga, J. Farrington-Zapata, S.G. Greenbaum, High pressure NMR study of water self-diffusion in Nafion-117 membrane , J. Phys. Chem. B 108 (2004) 4260–4262.
[12] A. Roy, M.A. Hickner, X. Yu, Y. Li, T.E. Glass, J.E. McGrath, Influence of chemical composition and sequence length on the transport properties of proton exchange membranes , J. Polym. Sci. B: Polym. Phys. 44 (2006) 2226–2239.
[13] J. Zhang, V. Giotto, W.-Y. Wen, A.A. Jones, An NMR study of the state of ions and diffusion in perfluorosulfonate ionomer , J. Membr. Sci. 269 (2006) 118–125.
[14] X. Guo, F. Zhai, J. Fang, M.F. Laguna, M. López-González, E. Riande, Permselectivity and conductivity of membranes based on sulfonated naphthalenic copolyimides , J. Phys. Chem. B. 111 (2007) 13694–13702.
[15] L. Garrido, J. Pozuelo, M. López-González, J. Fang, E. Riande, Simulation and experimental studies on proton diffusion in polyelectrolytes based on sulfonated naphthalenic copolyimides , Macromolecules 42 (2009) 6572–6580.
[16] K.D. Dorkenoo, P.H. Pfromm, M.E. Rezac, Gas transport properties of a series of high T_g polynorbornenes with aliphatic pendant groups , J. Polym. Sci. B: Polym. Phys. 36 (1998) 797–803.
[17] Y.P. Yampolskii, N.B. Bespalova, E.S. Finkelshtein, V.I. Bondar, A.V. Popov, Synthesis, gas permeability and gas sorption properties of fluorine containing norbornene polymers , Macromolecules 27 (1994) 2872–2878.
[18] M.A. Tlenkopatchev, E. Miranda, M.A. Canseco, R. Gaviño, T. Ogawa, Synthesis of a polynorbornene containing 3,5-di-ter-butyl-4-hydroxybenzoyl group , Polym. Bull. 34 (1995) 385–391.
[19] M.A. Tlenkopatchev, S. Fomine, L. Fomina, R. Gaviño, T. Ogawa, Ring-opening metathesis polymerization of coumarin containing norbornene , Polym. J. 29 (1997) 622–625.
[20] V.G. Maya, A.P. Contreras, M.A. Canseco, M.A. Tlenkopatchev, Synthesis and chromium complexation properties of an ionic polynorbornene , React. Funct. Polym. 49 (2001) 145–150.
[21] A.P. Contreras, M.A. Tlenkopatchev, M.M. López-González, E. Riande, Synthesis and gas transport properties of new high glass transition temperature ring-opened polynorbornenes , Macromolecules 35 (2002) 4677–4684.
[22] M.A. Tlenkopatchev, J. Vargas, M.M. López-González, E. Riande, Gas transport in polymers prepared via metathesis copolymerization of exo-*N*-phenyl-7-oxanorbornane-5,6-dicarboximide and norbornene , Macromolecules 36 (2003) 8483–8488.
[23] M. Tlenkopatchev, J. Vargas, M.A. Almaraz-Girón, M. López González, E. Riande, Gas sorption in new fluorine containing polynorbornenes with imide side chain groups , Macromolecules 38 (2005) 2696–2703.
[24] J. Pozuelo, M. López-González, M. Tlenkopatchev, E. Saiz, E. Riande, Simulations of gas transport in membranes based on polynorbornenes functionalized with substituted imide side groups , J. Membr. Sci. 310 (2008) 474–483.
[25] E.M. O'Connell, T.W. Root, S.L. Cooper, Morphological studies of lightly sulfonated polystyrene using Na-23 NMR. 1. Effects of sample composition , Macromolecules 27 (1994) 5803–5810.
[26] J. Vargas, A.A. Santiago, M.A. Tlenkopatchev, R. Gaviño, M.F. Laguna, M. López-González, E. Riande, Gas transport and ionic transport in membranes based on polynorbornenes with functionalized imide side groups , Macromolecules 40 (2007) 563–570.

[27] P.T. Callaghan, K.W. Jolley, C.M. Trotter, Stable and accurate spin echoes in pulsed field gradient NMR , J. Magn. Reson. 39 (1980) 525–527.
[28] E. Barsoukov, J.R. Macdonald (Eds.), Impedance Spectroscopy: Theory, Experiment and Applications, 2nd ed., Wiley, New Jersey, 2005 (Chapter 2).
[29] E.O. Stejskal, J.E. Tanner, Spin diffusion measurements: spin echoes in the presence of a time-dependent field gradient , J. Chem. Phys. 42 (1965) 288–292.
[30] L. Garrido, M. López-Gonzalez, E. Riande, Influence of local chain dynamics on diffusion of gases in polymers as determined by pulsed field gradient NMR , J. Polym. Sci. B: Polym. Phys. 48 (2010) 231–235.
[31] K. Díaz, L. Garrido, M. López-González, L.F. Del Castillo, E. Riande, CO_2 transport in polysulfone membranas containing zeolitic imidazolate frameworks as determined by permeation and PFG NMR techniques , Macromolecules 43 (2010) 316–325.
[32] J. Larminie, A. Dicks, Fuel Cell Systems Explained , 2nd ed., Wiley, West Sussex, England, 2003, p. 71.
[33] T. Sata, Ion-Exchange Membranes , Royal Society of Chemistry, Cambridge, 2004 (Chapter 2).